Excitation of Wakefields in Carbon Nanotubes and Graphene Layers: Hydrodynamic Model and PIC Simulations

P. Martín-Luna[1], A. Bonatto[2], C. Bontoiu[3], J. Rodríguez-Pérez[4], G. Xia[5], and J. Resta-López[4]

[1]Instituto de Física Corpuscular (IFIC), CSIC/UV, Paterna, Spain
[2]Universidade Federal de Ciências da Saúde de Porto Alegre, Porto Alegre, Brazil
[3]The University of Liverpool and Cockroft Institute, UK
[4]Instituto Universitario de Ciencia de los Materiales (ICMUV), Universidad de Valencia, Paterna, Spain
[5]The University of Manchester and Cockroft Institute, UK

Introduction

- **Carbon nanotubes (CNTs)** and **graphene layers** are **unique** for their size, shape, and physical properties, presenting the following **advantages** with respect to natural crystals:
  (i) transverse acceptances of the order of up to 100 nm [1] (i.e. three orders of magnitude higher than a typical silicon channel)
  (ii) larger degree of dimensional flexibility and thermomechanical strength
  (iii) lower dechannelling rate
  (iv) less disruptive effects such as filamentation and collisions

- Consequently, CNTs and graphene layers are considered robust candidates for solid-state or **plasmonic wakefield acceleration**.

Plasmonic acceleration

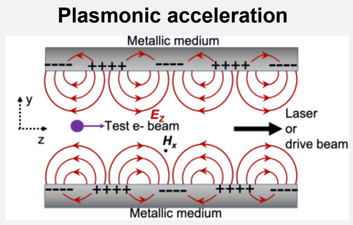

RF cavities

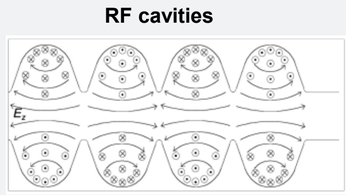

	Plasmonic acceleration	RF cavities
Aperture size	$\sim\mu$m	$\sim$cm
Length	$\sim$mm	~ 10 cm $-$ m
Longitudinal electric field	~ 100 GV/m	~ 100 MV/m
Operation	Travelling wave (TW)	Standing Wave (SW) or TW

Plasmonic wakefield acceleration

- ❑ Excitation of **surface plasmonic modes** [2-3] by laser (laser-driven) or charged particle beam (beam-driven)
- ❑ High-frequency collective oscillation of wall electrons
- ❑ Acting like a **structured plasma**
- ❑ To properly excite wakefields laser or beam driving parameters need to be in the time and space scale of the plasmon wave

Theoretical background

Linearized hydrodynamic model (LHM)

- In this theory [4-11], carbon nanostructures surfaces are modelled as an infinitesimally thin and infinitely long shells with uniform surface density n_0. These electrons are confined in the surfaces
- A driving charge Q travels with velocity v, parallel to the z-axis: $\mathbf{r_0} = (x_0, y_0, vt)$
- Position of electrons excited at the jth surface: $\mathbf{r_j}$

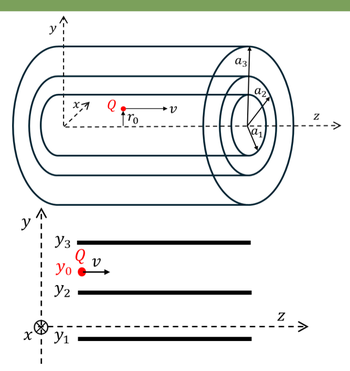

- The **electronic excitations** on the surfaces can be described by two differential equations:
  (i) the continuity equation

$$\frac{\partial n_j(\mathbf{r_j},t)}{\partial t} + n_0 \nabla_j \cdot \mathbf{u_j}(\mathbf{r_j},t) = 0$$

$n_j(\mathbf{r_j},t)$: perturbed surface density
$\mathbf{u_j}(\mathbf{r_j},t)$: velocity of the plasma
∇_j differentiates only tangentially to the jth surface

  (ii) the momentum-balance equation

$$\frac{\partial \mathbf{u_j}(\mathbf{r_j},t)}{\partial t} = \nabla_j \cdot \Phi(\mathbf{r_j},t) - \underbrace{\frac{\alpha}{n_0}\nabla_j \cdot n_j(\mathbf{r_j},t)}_{\text{Acoustic modes}} + \underbrace{\frac{\beta}{n_0}\nabla_j\left[\nabla_j^2 n_j(\mathbf{r_j},t)\right]}_{\text{Quantum correction}} - \underbrace{\gamma \mathbf{u_j}(\mathbf{r_j},t)}_{\text{Frictional force}}$$

$\alpha = v_F^2/2$, with $v_F = \sqrt{2\pi n_0}$ $\quad \beta = 1/4$

- The electric potential is given by $\Phi = \frac{Q}{\|\mathbf{r}-\mathbf{r_0}\|} + \Phi_{ind}$, where

$$\Phi_{ind}(\mathbf{r},t) = -\sum_j \int d^2\mathbf{r_j} \frac{n_j(\mathbf{r_j},t)}{\|\mathbf{r}-\mathbf{r_j}\|}$$

is the potential resulting from the perturbation of the electron fluids

- The system of partial differential equations can be analytically solved by using **Fourier transforms** [12]
- Induced wakefields:

$$W_x = -\frac{\partial \Phi_{ind}}{\partial x} \qquad W_y = -\frac{\partial \Phi_{ind}}{\partial y} \qquad W_z = -\frac{\partial \Phi_{ind}}{\partial z}$$

Results

Carbon nanotubes

PIC simulations

- The Fourier–Bessel Particle-in-Cell **(FBPIC)** code [13] is used to perform the simulations using a cylindrical CNT hollow plasma channel model employing 2D radial grids
- This code is based on a collisionless fluid model which does not take into account the solid-state properties related to the ionic lattice
- We define a hollow plasma channel model with inner radius r_{in} and wall thickness w_t with a volumetric density $n_V = 10^{28}$ m^{-3} of free electrons within this region

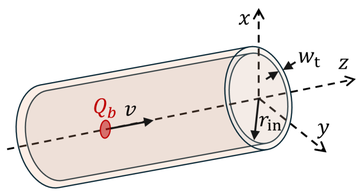

- We will consider a bi-Gaussian beam driver, with $\sigma_z = \sigma_r = 3.33$ nm, and charge $Q_b = -44$ fC with $v \to c$

Comparison

- We will assume that the number of free electrons in the cylindrical surface of radius $a = r_{in}$ and in the wall thickness w_t of the hollow plasma model is the same, obtaining the expression:

$$n_0 = \frac{n_V w_t}{2r_{in}}(2r_{in} + w_t)$$

- We define the plasma wavelength $\lambda_p = \frac{2\pi c}{\omega_p}$, where $\omega_p = \sqrt{e^2 n_V/\varepsilon_0 m_e}$ is the plasma frequency

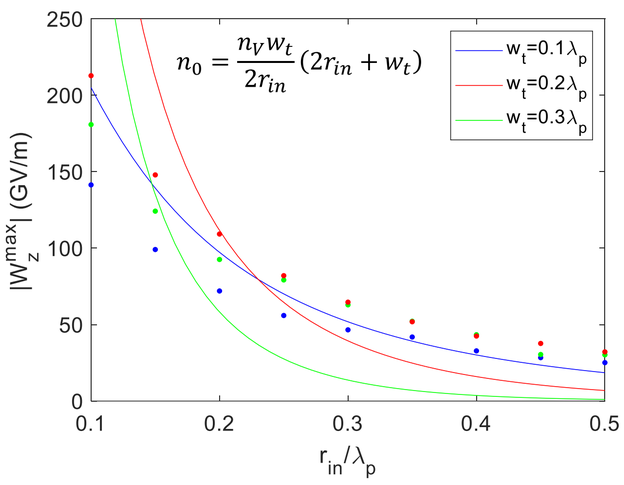

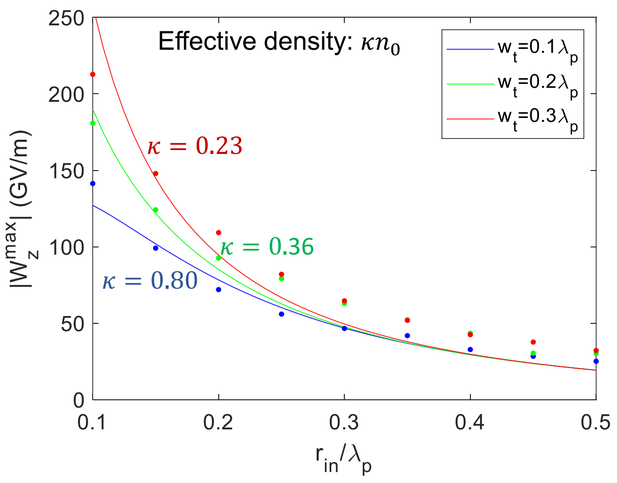

- There is a qualitatively good agreement in the amplitudes, in particular, for the smaller wall thickness $w_t = 0.1\lambda_p$, which is the most similar case of the theoretical model. The agreement is much better if we use an effective density that takes into account that not all electrons in the wall thickness excite the wakefield effectively

Graphene layers

PIC simulations

- **WarpX** [14] has been chosen to perform the simulations of the graphene layers
- Graphene layers are modelled as layers filled with a uniformly distributed, pre-ionized cold plasma of carbon ions and electrons
- Graphene layers will be centered at plane $y = y_j$ with a wall thickness w_t and a volumetric density $n_j = n_0/w_t$ in order to ensure that the number of free electrons within the jth layer with surface density $n_0 = 1.53 \times 10^{20}$ m^{-2} in the LHM is equal to the number of free electrons in the wall thickness w_t

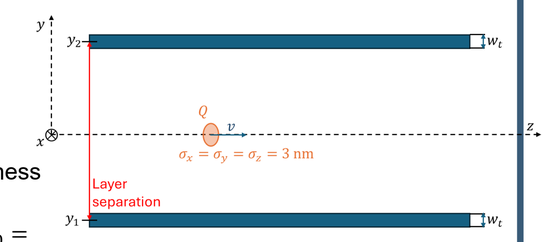

- We will consider a Gaussian proton beam as a driver, with $\sigma_x = \sigma_y = \sigma_z = 3$ nm, and charge $Q = 1000e$ travelling between the graphene layers
- The simulations span a total duration of 9.5 fs, which is sufficient for wakefield excitation to occur

Comparison

PIC simulations | Linearized hydrodynamic model

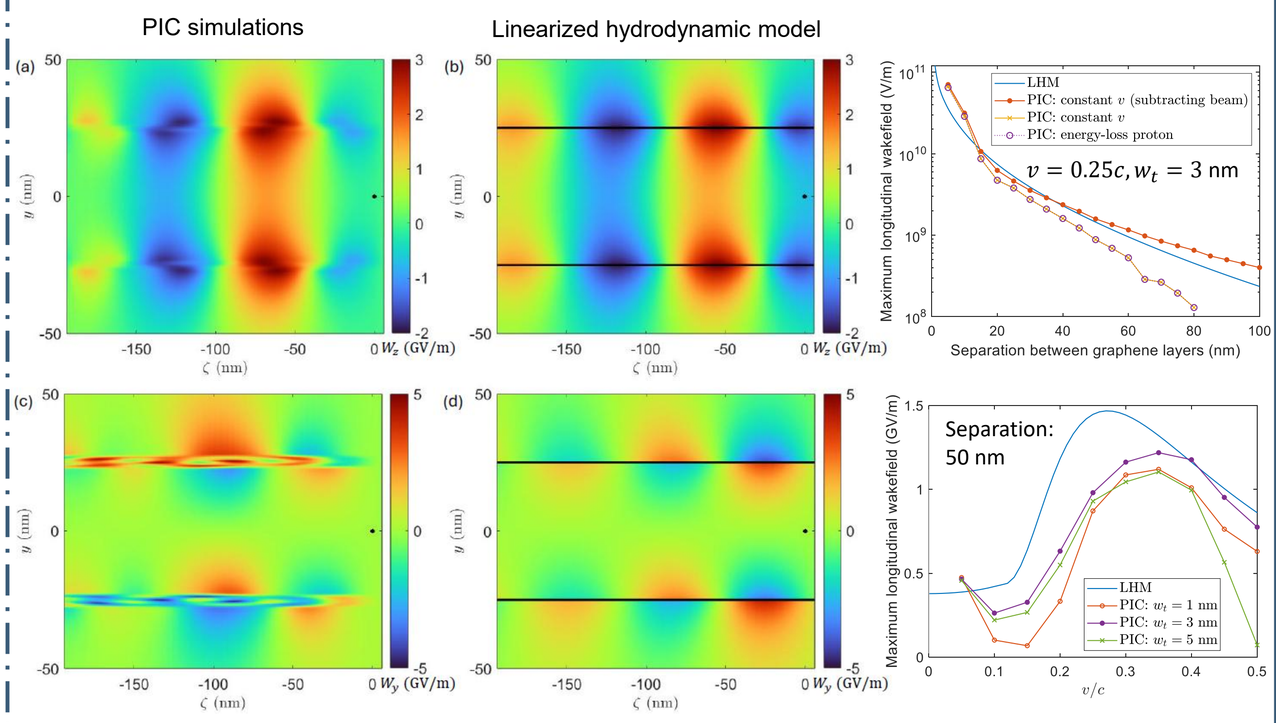

- In general, there is a good agreement between the PIC simulations and the linearized hydrodynamic model

Discussion

The **discrepancies** obtained between the linearized hydrodynamic model and the PIC simulations can be explained due to the differences between both approximations, such as:
- We are comparing a 3D region with free electrons in PIC simulations with 2D surfaces in the linearized hydrodynamic model
- The solid-state properties cannot be taken into account in PIC codes, whereas these properties may be modelled with the parameters α, β, and γ in the linearized hydrodynamic model
- The electrons and carbon ions comprising the CNT can move in 3D in PIC simulations, whereas they are assumed to be confined over the surface in the linearized hydrodynamic model
- The driver interacts with the surrounding medium (losing energy) in PIC codes, whereas in the linearized hydrodynamic model we assume a constant velocity
- The size of the driver beam in the PIC simulations is not a point-like charge as assumed in the linearized hydrodynamic model

Conclusions and forthcoming work

- We have compared the excited wakefields in carbon nanostructures using the **linearized hydrodynamic model** and PIC simulations
- The **amplitude** of the longitudinal wakefield follows a **similar trend** in the linearized hydrodynamic model and PIC simulations
- The agreement in the amplitude of the wakefield in CNTs is much better if we consider an **effective density**
- The linearized hydrodynamic model can be used to obtain an **estimation** of the amplitude of the wakefield in hollow plasmas with small wall thickness instead of performing time-consuming PIC simulations
- **Further investigations** employing a different approximation to relate the surface and volumetric density and scanning in other key parameters are ongoing

References

[1] Y.M. Shin et al., Nucl. Instrum. Meth. B **355**, pp. 94-100 (2015).
[2] M. S. Ukhtary and R. Saito, Carbon **167**, pp. 455-474 (2020).
[3] A. Macchi, Phys. Plasmas **25**, 031906 (2018).
[4] T. Stöckli et al., Phys. Rev. B **64**, 115424 (2001).
[5] Y.-N. Wang and Z. L. Mišković, Phys. Rev. A **69**, 022901 (2004).
[6] M. Nejati et al., Phys. Plasmas **16**, 022108 (2009).
[7] I. Radovic and D. Borka, Phys. Lett. A **374**, 1527-1533 (2010).
[8] P. Martín-Luna et al., New J. Phys. **25**, 123029 (2023).
[9] P. Martín-Luna et al., Res. Phys. **60**, 107698 (2024).
[10] P. Martín-Luna et al., J. Phys. D: Appl. Phys. **58**, 225203 (2025).
[11] P. Martín-Luna et al., Chin. J. Phys. **97**, 607-624 (2025).
[12] P. Martín-Luna and J. Resta-López, *Plasmonic Excitations in Carbon Nanostructures: Carbon Nanotubes Vs. Graphene at Electromagnetic Field - From Atomic Level to Engineering Applications. IntechOpen* (2025). DOI: 10.5772/intechopen.1009673
[13] R. Lehe et al., Comput. Phys. Commun**. 203**, 66–82 (2016).
[14] L. Fedeli et al. *Pushing the Frontier in the design of laser-based electron accelerators with groundbreaking mesh-refined particle-in-cell simulations on exascale-class supercomputers*. In: SC22: International Conference for High Performance Computing, Networking, Storage and Analysis. Dallas, Texas, USA: IEEE; 2022. pp. 1-12. DOI: 10.1109/SC41404.2022.00008

Corresponding author: **Pablo.Martin@ific.uv.es**

Work supported by the Ministerio de Universidades (Gobierno de España) under Grant Number FPU20/04958 and the Generalitat Valenciana under Grant Agreement CIDEGENT/2019/058.
ACKNOWLEDGEMENT - This poster presentation has received support from the European Union's Horizon 2020 Research and Innovation programme under Grant Agreement No 101004730.

https://www.uv.es/resta/NOVAS/Home.html